Optical Absorption Spectra of Chromium-Doped Zinc Sulfide Crystals*

C. Stuart Kelley and Ferd Williams
Physics Department, University of Delaware, Newark, Delaware 19711
(Received 5 May 1969; revised manuscript received 26 January 1970)

We have measured the optical absorption spectra of twinned cubic crystals of chromium-doped zinc sulfide between 5000 and 29 000 cm^{-1} (2–0.34 μm) at 4.2–500°K. Two broad absorption bands are specific to chromium; at 77°K, one has a maximum at 24 400 cm^{-1}, the other, at 5700 cm^{-1}. Weak photoconductivity is observed in the former; but none in the latter. Twelve narrow bands between 5100 and 5250 cm^{-1} are identified as zero-phonon transitions in Cr^{+2} ($3d^4$) substitutional at cation sites, two for the cubic structure, ten for the twin boundaries. The cubic crystal field is determined. Thirteen phonon-assisted transitions are identified and the phonon wave numbers are evaluated. We propose that the 24 400-cm^{-1} band involves transitions to the conduction band edge.

I. INTRODUCTION

Most studies of Cr in II–VI compounds have involved ESR measurements.[1-4] Although optical absorption studies have been reported for Cr^{+2} ($3d^4$) in solution as well as in crystals,[5,6] the only II–VI crystals investigated were cadmium sulfide. The broad infrared optical absorption in CdS:Cr has been attributed to the transition between crystal field split levels of the Cr^{+2} ground state (^5D). No fine structure was reported at liquid-helium temperature.[6] Unstructured emission at 5000 cm^{-1} in ZnS:Cr has been reported.[7]

Optical absorption measurements have not been previously reported for ZnS:Cr. One would expect absorption bands appropriate to Cr^{+2} at cation sites. In tetrahedral coordination, the free-ion Cr^{+2} ground state splits into a ^5E level and a $^5T_2$ level (ground state) separated by the crystal field parameter Δ_t. For Cr^{+2} in octahedral coordination with H_2O ligands,[5] $\Delta_0 = 13\,900$ cm^{-1}; for tetrahedral symmetry, $\Delta_t = -\frac{4}{9}\Delta_0 \simeq -6200$ cm^{-1}. In going from H_2O to sulfide coordination, Δ_t may be further reduced.[6] Therefore, the $^5T_2 \rightarrow {}^5E$ transition is expected in the near infrared. Effects of higher-lying Cr^{+2} states may be disregarded since they occur above 16 000 cm^{-1}. The $^5T_2$ and ^5E spin-orbit splittings are small compared to the crystal field splitting, the larger in the $^5T_2$ than in the ^5E. The transition probabilities[8] for transitions between the spin-orbit levels allow prediction of the optical absorption spectrum.

II. EXPERIMENTAL

A. Samples

Preparation of the ZnS:Cr single crystals has been described elsewhere.[9] Basically, the crystals were grown from the vapor phase using a self-sealing method. Dopant was added as either chromic chloride, chromic sulfide, or chromium metal. Transport of chromium to the growing crystal was more efficient for the chloride and the sulfide, and the resulting crystals have higher chromium concentrations than those prepared with metal dopants (Table I). The crystals were sliced and mechanically polished. As determined by spectrochemical analysis, chromium is the dominant impurity. The crystal structure was determined by x-ray measurements for one sample of each of the variously doped crystals (e.g., from $CrCl_3$, Cr_2S_3, or Cr metal) prior to annealing. All samples were found to be cubic, but with some twinning. The crystals were annealed under various conditions. Along with small amounts of zinc or sulfur sufficient to produce the required zinc pressures, crystals were sealed in evacuated quartz ampoules. After 48 h at 900 °C the ampoules were withdrawn from the oven and quenched in water.

B. Apparatus

Optical absorption measurements were performed with a Model 14R Cary recording spectrophotometer. For 4.2 °K measurements, crystals were immersed in liquid helium in a glass Dewar. For $6.0 \leq T \leq 77$ °K, they were mounted on the cold finger of a Sulfrian variable temperature cryostat. For $T > 77$ °K, the crystals were mounted in a Hoffman research cryostat. In all cases, heating was electrically controlled. A copper-constantan

TABLE I. Impurity concentrations of single crystals of ZnS used for optical absorption measurements.

Crystal	Preparation method	Impurity (in parts per million) Cr	Fe	Cu	Ga	Mn	Mg
C	$CrCl_3$	470	20	2	<50	~1.0	10-100
S	Cr_2S_3	160	20	3	<50	0.1-1.0	1.0-10
M	Cr metal	31	1.0	1.5	<50	0.1-1.0	<1.0

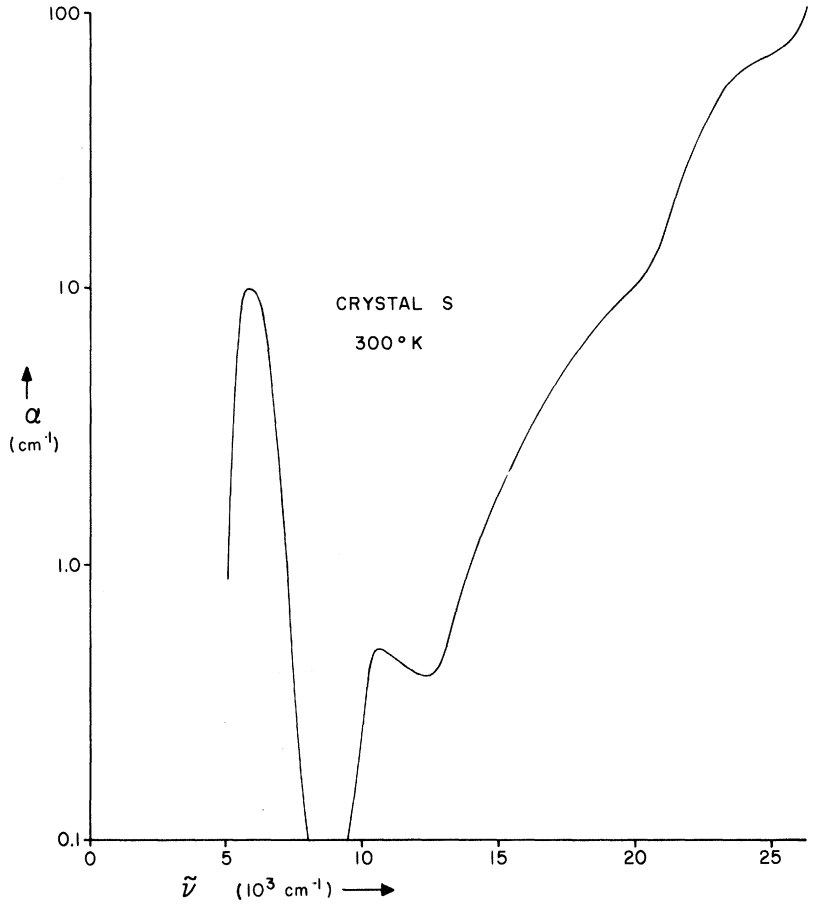

FIG. 1. Optical absorption coefficient α versus photon wave number $\tilde{\nu}$ at 300 °K for crystal S of twinned cubic ZnS: Cr.

thermocouple mounted between the crystal and the cold finger was used for $T > 77$ °K; for $T \leq 77$ °K, a gold-doped germanium crystal was employed.

III. EXPERIMENTAL RESULTS

The optical absorption spectrum between 5000 and 29 000 cm^{-1} (2–0.34 μm) of the ZnS:Cr crystal consists of three broad bands (Fig. 1).

The intensity of the 5700-cm^{-1} band increases linearly with chromium concentration. The oscillator strength is 5×10^{-3} and temperature independent over 4.2-500 °K. No photocurrent has been found to accompany this absorption. Below 37 °K fine structure (Fig. 2) is observed which is dependent on chromium concentration and independent of the method of doping, whether by $CrCl_3$, Cr_2S_3, or Cr metal.

Temperature dependences of the five most intense lines in Fig. 3 were monitored over 4.2–44 °K. The logarithms of the peak absorption coefficient α_m for each of these absorptions decrease linearly with increasing T. All other lines in Fig. 3 display the same dependence. By immersing the crystals in liquid helium, spectra similar to those shown in Figs. 1–3 are obtained, except for enhanced line intensities. The wave numbers and oscillator strengths of peaks 1–12 at 7.2 °K are listed in Table II along with the broader peaks 13–25. To investigate the dependences of peaks 1–12 on annealing conditions, the crystals were annealed at various zinc pressures (Table III). The density of twin boundaries as a function of P_{Zn} has a minimum near the vacuum anneal (10^{-4} atm). This is because fewer defects are incorporated at this pressure.[10] The intensities of zero-phonon lines originating from Cr^{+2} at twin boundaries were expected to reflect this dependence. Absorption measurements were performed at 7.2 °K after each anneal and the line intensities were obtained. The behavior of these intensities formed two groups. One group, type A, was composed of lines 10 and 11, whose behaviors are more consistent with each other than with lines of type B, which was composed of the rest of the lines. That part of the total intensity, $f_A = I_A/(I_A + I_B)$ and $f_B = I_B/(I_A + I_B)$, versus P_{Zn} is given in Table III for each type.

During the growth of the crystals, manganese was introduced as an impurity (Table I). The Mn^{+2} ESR signal has been used as a structure indicator in doped ZnS.[11] Therefore, prior to the heat treat-

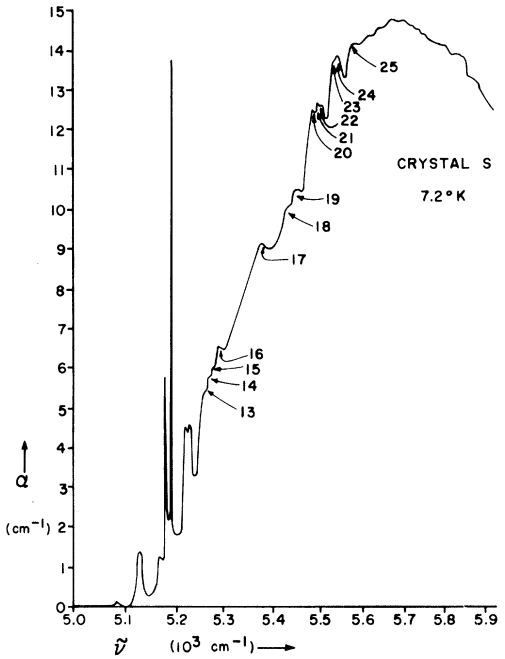

FIG. 2 Optical absorption coefficient versus photon wave number for crystal S at 7.2 °K on an expanded scale. Numbered peaks identify phonon-assisted peaks and are assigned in Table II.

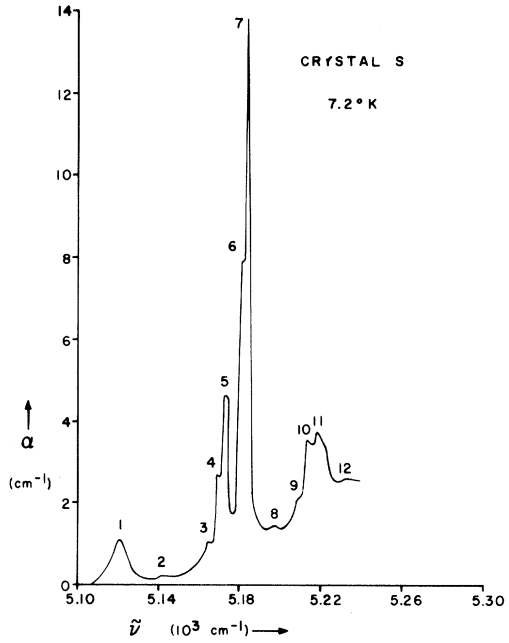

FIG. 3. Optical absorption coefficient versus photon wave number for crystal S at 7.2 °K on an expanded scale showing the zero-phonon wave numbers.

ments, one piece of a crystal was broken off and annealed with the larger samples. ESR measurements of Mn^{+2} in this piece were obtained before and after each anneal. Because twin boundary sites have hexagonal structure up to third nearest neighbors, the Mn^{+2} spectrum due to these sites is not expected to differ substantially from that due to hexagonal sites. The fractions of the total ESR signal intensity (Table III, as defined above) for cubic and twin boundary signals are considered, respectively, measures of the density of cubic sites and of the density of twinned sites.

A broad absorption band of very weak intensity is located at 11 000 cm^{-1}. Its intensity is diminished by a factor of 10 in undoped crystals, while the 5700-cm^{-1} band diminishes by at least a factor of 10^3. This peak is not attributed to Cr^{+2}.

Near the fundamental absorption edge, there is an absorption band with maximum at 24 400 cm^{-1} (shown in Fig. 4 along with an undoped crystal) and an oscillator strength of 8.8×10^{-2} at 77 °K. The intensity is dependent on chromium concentration and independent of the method of doping. Weak photocurrent accompanies this absorption. The absorption is resolved by lowering the temperature from 300 to 77 °K. As the temperature is further lowered to 7.2 °K, no structure appears and the band has roughly the same shape as at 77 °K.

TABLE II. Observed wave numbers and oscillator strengths, and assignments of fine structure in the Cr^{+2} $^5T_2 \rightarrow {}^5E$ absorption band at 7.2 °K. The evaluated wave numbers for the vibrational modes of cubic ZnS are listed.[a]

Absorption	Wave number $\tilde{\nu}$ (cm^{-1})	Assignment	Oscillator strength (in 10^{-6})
1	5123.5		17.3
2	5158.6		<1.0
3	5163.2		3.9
4	5168.5		8.7
5	5172.2		15.2
6	5179.5		13.9
7	5182.2		37.3
8	5195.9		1.0
9	5208.1		<1.0
10	5213.5	$\Gamma_4 \rightarrow \Gamma_2$	11.1
11	5219.2	$\Gamma_4 \rightarrow \Gamma_4$, Γ_1-Γ_5	12.2
12	5231.2		1.4
13	5250.7	2+TA	
14	5257.6	3+TA	
15	5267.9	5+TA	
16	5278.4	7+TA	
17	5366.8	7+LA	
18	5422.4	5+2 TA	
19	5438.3	7+2 TA	
20	5470.5	3+TO	
21	5482.5	5+TO	
22	5493.6	7+TO	
23	5513.9	5+LO	
24	5523.3	7+LO	
25	5561.1	7+3 TA	

[a] TA = 111 ± 13 cm^{-1}, LA = 185 ± 1 cm^{-1}, TO = 310 ± 2 cm^{-1}, LO = 341.4 ± 0.3 cm^{-1}.

TABLE III. Ratios R_A, R_B, R_c, and R_t after annealing at five zinc pressures.

P_{Zn}	$f_A = \frac{I_A}{I_A+I_B}$	$f_B = \frac{I_B}{I_A+I_B}$	$f_c = \frac{I_c}{I_c+I_t}$	$f_t = \frac{I_t}{I_c+I_t}$
3.2×10^{-7}	0.12	0.88	0.93	0.074
2.0×10^{-6}	0.17	0.83	0.94	0.056
1.1×10^{-5}	0.21	0.79	0.94	0.057
5.8×10^{-5}	0.30	0.70	0.94	0.059
4.0×10^{-2}	0.20	0.80	0.93	0.067
1.0	0.21	0.79	0.94	0.058

IV. INTERPRETATION

On the basis of the widths of the fine structure, the absorption spectrum may be divided into two regions; for $\tilde{\nu} \leq 5250$ cm^{-1} the absorptions consists of narrow peaks whereas for $\tilde{\nu} > 5250$ cm^{-1} the peaks are broader. The former are considered to be zero-phonon absorptions. They represent transitions which neither create nor destroy phonons. The latter are considered to be phonon-assisted absorptions, where creation of phonons accompanies the zero-phonon transitions.

The linear decrease of $\ln(\alpha_m)$ for each zero-phonon line with increasing temperature is consistent with transitions arising from a single initial state at a single center, several initial states at a single center lying within kT of each other at the lowest temperature (4.2 °K), or several initial states at several centers.

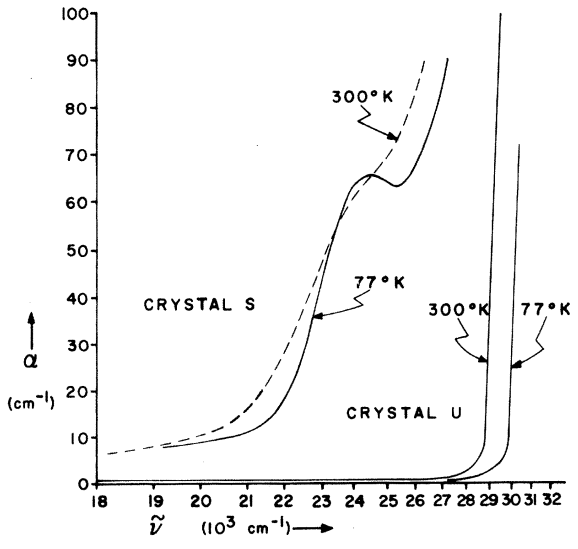

FIG. 4. Optical absorption coefficient versus photon wave number for Cr-doped (S) and -undoped (U) ZnS single crystals at 77 and 300 °K. At 4.2 °K, the spectra are similar to those at 77 °K. The 24 400-cm^{-1} band shows no fine structure.

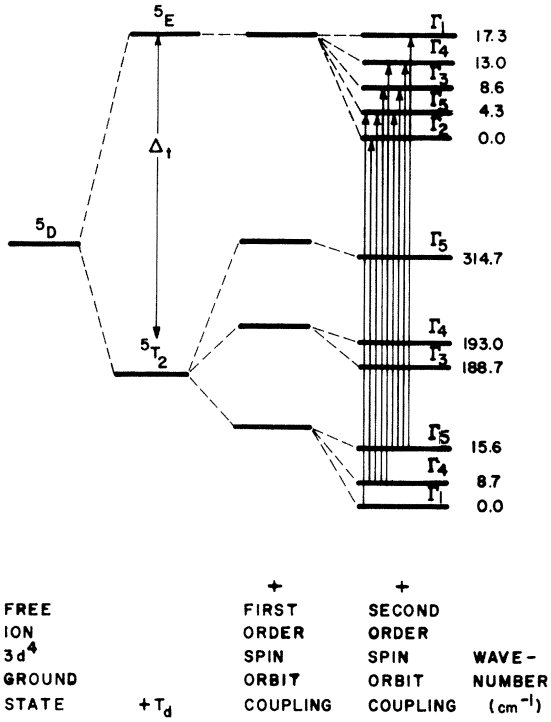

FIG. 5. Energy levels of tetrahedrally coordinated Cr^{+2} ($3d^4$) as predicted by crystal field theory. Allowed electric dipole transitions and wave numbers of energy levels are shown.

The zero-phonon absorptions may be attributed to Cr^{+2} at cation sites (a) in the cubic structure, (b) at twin boundaries, or (c) associated with crystal defects. These possibilities will now be examined.

Although there is scatter in the annealing data (Table III), there is a correlation between f_A and f_c. On this basis, absorption lines 10 and 11 are considered to originate from Cr^{+2} at cation sites in the cubic structure. To second-order spin-orbit interaction, the $^5T_2$ is split into six unevenly spaced levels, the ^5E into five evenly spaced levels[12] (Fig. 5). Assigning $\Delta_t = -5000$ cm^{-1} and retaining the free-ion spin-orbit coupling constant $\lambda = 58$ cm^{-1}, the second and third lowest $^5T_2$ states lie 8.7 and 15.6 cm^{-1} above the ground state. The interval between levels of the ^5E state is 4.3 cm^{-1}. Allowed electric dipole transitions are shown in Fig. 5, and their relative strengths are displayed in Table IV. Indentifying absorption line 10 as the $\Gamma_4 - \Gamma_2$ transition and retaining the free-ion spin-orbit coupling constants, the crystal field parameter is $\Delta_t = -5090 \pm 15$ cm^{-1}. The indeterminancy is due to uncertainty in λ, which may possibly be altered by 10% of the free-ion value.[8] This value of Δ_t is lower than those found in the literature.[5,6] The reason is that previous authors

TABLE IV. Wave numbers and intensities of allowed electric dipole transitions between spin-orbit levels of $^5T_2$ and ^5E at 7.2 °K as predicted from crystal field theory.

Transition	$\Delta\nu$ (cm^{-1})	Intensity (arbitrary units)
$\Gamma_1 \rightarrow \Gamma_5$	15.6	200
$\Gamma_4 \rightarrow \Gamma_4$	15.6	51.0
$\Gamma_5 \rightarrow \Gamma_1$	13.0	21.6
$\Gamma_4 \rightarrow \Gamma_3$	11.2	25.5
$\Gamma_5 \rightarrow \Gamma_4$	8.7	7.2
$\Gamma_4 \rightarrow \Gamma_5$	6.9	17.0
$\Gamma_5 \rightarrow \Gamma_3$	4.3	10.8
$\Gamma_4 \rightarrow \Gamma_2$	3.6	51.0
$\Gamma_3 \rightarrow \Gamma_5$	0	2.40

identified Δ_t with the broad band maximum. Absorption line 11 is identified with the coincident $\Gamma_1 \rightarrow \Gamma_5$ and $\Gamma_4 \rightarrow \Gamma_4$ transitions.[13]

The zero-phonon lines of type *B* are not considered as due to Cr-defect associates because of the narrow spread (108 cm^{-1}) of the lines, which indicates tetrahedrally coordinated Cr^{+2} subjected to a rather small perturbation. This can be provided by the crystal field at the twin boundaries. The twinned cubic structure is identical to the hexagonal structure up to third nearest neighbors. However, it is the same as the cubic structure only up to second nearest neighbors. This slight distortion of the regular cubic structure is proposed to result in absorption lines of type *B*. The annealing data support this identification.

Wave numbers of absorption lines believed to represent phonon-assisted transitions are displayed in Table II, along with their assignments. The phonons are assigned specific energies because principal contributions arise from those parts of the phonon spectra having maximum densities of states. We shall refer to these specific energies as the phonon energies. Because of the low temperature (7.2 °K), the phonon processes consist only of phonon emission. Thirteen bands can be identified as zero-phonon transitions combined with one or more of the four phonon wave numbers: 111 ± 13 cm^{-1}, 185 ± 1 cm^{-1}, 310 ± 2 cm^{-1}, and 341.4 ± 0.3 cm^{-1}. The indeterminancy stems from that range needed to explain the slightly different peaks. Surveys of results obtained by other authors are available.[8,14] Values averaged from the literature for phonon wave numbers in cubic zinc sulfide are TA = 115 cm^{-1}, LA = 184 cm^{-1}, TO = 296 cm^{-1}, and LO = 331 cm^{-1}.

The 24 400-cm^{-1} absorption band is attributed to transitions from $^5T_2$ levels to the conduction band edge, and not to levels derived from free-ion excited states (^3P, ^3H, etc.). The photoconductivity associated with this absoprtion is the most direct evidence. It is understandable that the photoconductivity is weak because substitutional Cr^{+2} is an electron trap, forming Cr^{+1} whose spin resonance is well known.[15] Also, the ground state of substitutional Fe^{+2} is believed to lie within 1 eV of the valence band edge.[16] From similarities between Cr^{+2} and Fe^{+2} (for example, their free-ion ionization energies differ by only 0.3 eV), the probable energy of the $^5T_2$ level of Cr^{+2} with respect to the band structure is consistent with our identification of the 24 400-cm^{-1} absorption. Also, the oscillator strength of $\frac{1}{10}$ and lack of fine structure are consistent with a transition to a continuum.

V. CONCLUSIONS

The near-infrared absorption in chromium-doped zinc sulfide crystals is explained by Cr^{+2} at substitutional cation cites in the cubic regions and at twin boundaries. From the low-temperature fine structure, zero-phonon and phonon-assisted transitions are identified, the cubic crystal field parameter and the phonon wave numbers evaluated. The near band-edge absorption is attributed to transitions from Cr^{+2} to the conduction band.

ACKNOWLEDGMENTS

We are pleased to acknowledge useful discussions with Dr. G. A. Slack and Dr. J. Vallin. We are also indebted to R. B. Lauer for growing the crystals, to P. J. DiBona for performing the ESR measurements, and to Professor R. B. Murray and his students for cooperation on measurements made with the Cary.

---

*Work supported by a grant from the Army Research Office (Durham); part of work submitted for the Ph. D. degree by C. S. K.

[1]R. S. Title, Phys. Rev. 133, A1613 (1964).

[2]T. L. Estle, G. K. Walters, and M. deWit, Paramagnetic Resonance 1, 144 (1963).

[3]K. Morigaki, J. Phys. Soc. Japan 19, 187 (1964).

[4]G. W. Ludwig and M. R. Lorenz, Phys. Rev. 131, 601 (1963).

[5]Y. Tanabe and S. Sugano, J. Phys. Soc. Japan 9, 753 (1954); 9, 766 (1954).

[6]R. Pappalardo and R. E. Dietz, Phys. Rev. 123, 1188 (1961).

[7]H. Nelkowski and G. Grebe, J. Luminescence 1, 88 (1970).

[8]G. A. Slack, F. S. Ham, and R. M. Chrenko, Phys. Rev. 152, 376 (1966).

[9]Indradev and R. B. Lauer, Mater. Res. Bull. 1, 185 (1966).

[10]W. Roth, in *Physics and Chemistry of* II-VI *Com-*

pounds, edited by M. Aven and J. S. Prener (Wiley, New York, 1967), p. 119.
[11]M. Aven and J. A. Parodi, J. Phys. Chem. Solids 13, 56 (1960).
[12]W. Low and M. Weger, Phys. Rev. 118, 1119 (1960); 118, 1330 (1960).
[13]Recent work by J. Vallin and G. A. Slack indicates that two lines close to 10 and 11 originate from cubic sites (unpublished).
[14]W. G. Spitzer, in *Semiconductors and Semimetals*, edited by R. K. Willardson and A. C. Beer (Academic, New York, 1967), Vol. 3, p. 17.
[15]H. D. Fair, Jr., R. D. Ewing, and F. E. Williams, Phys. Rev. 144, 298 (1966).
[16]F. E. Williams, in *International Symposium on Luminescence*, edited by N. Riehl and H. Kallmann (Thiemig, Munich, 1965), p. 332.

PHYSICAL REVIEW B VOLUME 2, NUMBER 1 1 JULY 1970

Theoretical Study of the Raman Relaxation of Ni^{2+} and Cr^{3+} Ions in MgO Crystals

D. K. Ray and T. Ray
Faculté des Sciences, Laboratoire de Spectromètrie Physique, Cedex 53, 38-*Grenoble, France*
and
M. J. L. Sangster
J. J. Thomson Physical Laboratory, Reading, United Kingdom
and
S. K. Gupta
Saha Institute of Nuclear Physics, Calcutta-9, *India*
(Received 11 November 1969)

The Raman relaxation rates for Ni^{2+} and Cr^{3+} ions in MgO crystals have been calculated using a shell model of phonons which is in good agreement with the results of neutron scattering experiments. These shell-model results are compared with those obtained with the Debye model for the phonons and, also, with the available experimental results for Ni^{2+} and Cr^{3+} in MgO. In the case Ni^{2+}, 50 °K is the highest temperature for which the relaxation time is sufficiently long to be directly measureable. As might be expected, in this low-temperature region the results based on the shell model and the Debye model of phonons are not significantly different. However, the values of relaxation rates at 123 and 136 °K obtainable from the recent line-shape measurements for Ni^{2+} in MgO are in good agreement with those calculated on the basis of the shell model of phonons. In the case of Cr^{3+} ions, the relaxation time can be measured directly up to temperatures as high as 200 °K, and in this range of temperature the two sets of results differ considerably. With the shell model, we obtain good agreement with the experimental results on the functional dependence of the relaxation rate $1/T_1$ on temperature. However, the absolute values of $1/T_1$ for Cr^{3+} obtained with this phonon model are on the average less than the experimental measurements by a factor of 5. The possible sources which might be important in bridging the gap between the theoretical and experimental results are discussed.

I. INTRODUCTION

It is well known that when spin-resonance transitions are induced in a paramagnetic crystal by applying external microwave power, the spin system then relaxes through the dissipation of energy to the lattice. In the single-phonon process, the spin-lattice relaxation amounts to the creation of phonons of energy equal to the energy of the spin transitions, whereas, in the only important two-phonon process, two phonons simultaneously take part – one being annihilated and another being creating, conserving the net energy. Obviously, in the two-phonon process, the entire phonon spectrum will be involved and consequently, at higher temperatures, two-phonon processes are expected to be important in the relaxation mechanisms. The relative importance of the high-frequency phonons will depend on the temperature at which the relaxation is measured. Most paramagnetic ions have relaxation times too short to be measured directly above the liquid-nitrogen temperature, so that only the effects of phonons of relatively small frequencies (<100 cm^{-1}) can be studied by means of resonance techniques. In explaining the data from the specific heat experiments, the Debye model is found to give a fairly good description of the low-frequency phonons.[1] Hence,